RNF17, a component of the mammalian germ cell nuage, is essential for spermiogenesis

Jieyan Pan[1], Mary Goodheart[2], Shinichiro Chuma[3], Norio Nakatsuji[3], David C. Page[2] and P. Jeremy Wang[1,*]

[1]Department of Animal Biology, School of Veterinary Medicine, University of Pennsylvania, Philadelphia, PA 19104, USA
[2]Howard Hughes Medical Institute, Whitehead Institute, and Department of Biology, Massachusetts Institute of Technology, 9 Cambridge Center, Cambridge, MA 02142, USA
[3]Institute for Frontier Medical Sciences, Kyoto University, Sakyo-ku, Kyoto 606-8507, Japan
*Author for correspondence (e-mail: pwang@vet.upenn.edu)

Accepted 18 July 2005

Development 132, 4029-4039
Published by The Company of Biologists 2005
doi:10.1242/dev.02003

Summary

Nuages are found in the germ cells of diverse organisms. However, nuages in postnatal male germ cells of mice are poorly studied. Previously, we cloned a germ cell-specific gene named *Rnf17*, which encodes a protein containing both a RING finger and tudor domains. Here, we report that RNF17 is a component of a novel nuage in male germ cells – the RNF17 granule, which is an electron-dense non-membrane bound spherical organelle with a diameter of 0.5 μm. RNF17 granules are prominent in late pachytene and diplotene spermatocytes, and in elongating spermatids. RNF17 granules are distinguishable from other known nuages, such as chromatoid bodies. RNF17 is able to form dimers or polymers both in vitro and in vivo, indicating that it may play a role in the assembly of RNF17 granules. *Rnf17*-deficient male mice were sterile and exhibited a complete arrest in round spermatids, demonstrating that *Rnf17* encodes a novel key regulator of spermiogenesis. *Rnf17*-null round spermatids advanced to step 4 but failed to produce sperm. These results have shown that RNF17 is a component of a novel germ cell nuage and is required for differentiation of male germ cells.

Key words: *Rnf17*, Nuage, Tudor, RING, Spermiogenesis, Mouse

Introduction

Spermatogenesis, the elaborate process by which sperm are produced, is marked by dramatic cell proliferation and differentiation (Russell et al., 1990; Sharpe, 1993). Spermatogenesis can be divided into three phases: mitotic, meiotic and haploid. During the mitotic phase, stem cell spermatogonia undergo self-renewal, proliferation and differentiation. Eventually spermatogonia enter meiosis to become spermatocytes. During meiosis, DNA replicates only once so that two successive rounds of meiotic cell divisions result in haploid spermatids. Homologous chromosome synapsis and recombination occur during the prophase of the first meiotic cell division, which is further divided into five stages: preleptotene, leptotene, zygotene, pachytene and diplotene. During the haploid phase, spermatids undergo complex differentiation and morphogenesis processes, including acrosome formation, chromatin condensation, cytoplasm elimination and flagellum development. One of the striking features of spermatogenesis is that dividing germ cells are interconnected by stable cytoplasmic bridges because of incomplete cytokinesis (Fawcett et al., 1959).

Nuage is found in germ cells of diverse organisms (al-Mukhtar and Webb, 1971; Eddy, 1974; Mahowald, 1968). The term nuage refers to various forms of electron-dense cellular material that are amorphous and are not surrounded by membranes. The most extensively characterized nuage is the *Drosophila* polar granule (Mahowald, 1968). The polar granule is present in the cytoplasm of oocytes and is required for germ cell specification during embryogenesis (Mahowald, 2001). Components of polar granules include Tudor and Vasa (Bardsley et al., 1993; Hay et al., 1988; Thomson and Lasko, 2004). The *Drosophila* Tudor protein contains 10 copies of what has been termed the tudor domain. The function of tudor domain is unknown (Ponting, 1997).

The mouse Vasa homolog (MVH) is a component of chromatoid bodies in mammalian germ cells (Toyooka et al., 2000). MVH is required for spermatogenesis in mice (Tanaka et al., 2000). The chromatoid body is a prominent multi-lobular nuage found in the cytoplasm of spermatocytes and spermatids (Eddy, 1970; Sud, 1961a). The function of chromatoid bodies is not known. Interestingly, mouse TDRD1 (also referred to as MTR-1), containing four tudor domains, is also a component of the chromatoid body (Chuma et al., 2003). In addition to the chromatoid body, early ultrastructural studies identified as many as five other types of nuage in rat male germ cells, including chromatoid satellites, sponge bodies and spherical particles (Fawcett et al., 1970; Russell and Frank, 1978). Frequently, little distinction is made between these lesser known nuages and chromatoid bodies, largely owing to a lack of specific cytological markers that might distinguish among them.

Recent microarray analyses have shown that haploid germ cells express a far greater number of germ cell-specific genes than spermatogonia and spermatocytes (Schultz et al., 2003; Shima et al., 2004). By contrast, only five mutants generated by gene targeting caused complete arrest in spermiogenesis, in

which spermatids failed to produce spermatozoa. These five genes [*Crem*, *Miwi* (*Piwil1* – Mouse Genome Informatics), *Trf2* (*Tbpl1* – Mouse Genome Informatics), *Tpap* (*Papolb* – Mouse Genome Informatics) and *Ddx25*] constitute a unique group of so-called 'key regulators of spermiogenesis' (Blendy et al., 1996; Deng and Lin, 2002; Kashiwabara et al., 2002; Martianov et al., 2001; Nantel et al., 1996; Tsai-Morris et al., 2004; Zhang et al., 2001). CREM is a transcriptional activator (Blendy et al., 1996; Nantel et al., 1996). MIWI is a cytoplasmic protein and is associated with mRNAs (Deng and Lin, 2002). Disruption of *Crem* or *Miwi* results in arrest of round spermatids at step 4. TRF2 is a TBP (TATA-binding protein)-related transcription factor (Martianov et al., 2001; Zhang et al., 2001). TPAP is a testis-specific cytoplasmic poly(A) polymerase (Kashiwabara et al., 2002). Spermiogenesis proceeds up to step 7 in mice that lack either TRF2 or TPAP. DDX25 is a testicular RNA helicase. Lack of DDX25 causes round spermatid arrest at step 8 (Tsai-Morris et al., 2004). These key regulators appear to define distinct regulatory pathways of spermiogenesis, even though they may regulate some common target genes or transcripts. They share two common features. First, the arrest of spermiogenesis is complete and uniform in mutant mice. Second, each key regulator affects the transcription or translation of multiple (even hundreds of) genes or transcripts, suggesting that they function as 'master switches' of spermiogenesis.

Here, we describe studies of a novel key regulator of spermiogenesis called *Rnf17*. We previously showed that *Rnf17* is specifically expressed in testis (Wang et al., 2001). RNF17 contains a RING finger motif and tudor domains. The RING finger motif is present in many ubiquitin E3 ligases (Joazeiro and Weissman, 2000; Lorick et al., 1999). RNF17 interacts with all four members of the Mad family (Mad1, Mxi1, Mad3 and Mad4), which are basic-helix-loop-helix-leucine zipper (bHLH-ZIP) transcription factors of the Myc oncoprotein network (Yin et al., 1999). Mad proteins repress transcription of Myc-responsive genes by binding to Max (a bHLH-ZIP protein). Mad-Max heterodimers compete with Myc-Max heterodimers for the same 'myc box sequence' CAC/TGTG in the Myc-responsive genes (Grandori et al., 2000). RNF17 was able to activate transcription of Myc-responsive genes by recruiting Mad proteins from the nucleus to the cytoplasm (Yin et al., 2001; Yin et al., 1999). In this report, we identify RNF17 as an integral component of the RNF17 granule, a novel nuage in male germ cells. RNF17 forms a complex with itself. We disrupted *Rnf17* in mice by gene targeting and found that animals lacking *Rnf17* were viable but male sterile. The *Rnf17*-deficient testis displayed a complete arrest in spermiogenesis.

Materials and methods

Cloning of *Rnf17* cDNAs

Based on previously reported *Rnf17* cDNA sequences, we designed *Rnf17*-specific primers for 3′RACE to obtain full-length cDNA sequences for *Rnf17s* and *Rnf17l* (Wang et al., 2001; Yin et al., 1999). By using 3′RACE (rapid amplification of cDNA ends), we amplified, subcloned and sequenced *Rnf17* cDNA fragments from bulk mouse testis Marathon-Ready cDNAs (BD Biosciences). The composite cDNA sequences have been deposited in GenBank under the following accession numbers: *Rnf17s*, AY854010; *Rnf17l*, AY854011.

Generation of antibodies

Two polyclonal anti-RNF17 antibodies were generated. The *Rnf17* cDNA fragment encoding the N-terminal 100 residues was cloned into pGEX-4T-1 (Amersham Biosciences). The GST-RNF17 (1-100) fusion protein was expressed in BL21 bacteria, purified with glutathione-sepharose beads and used to immunize two rabbits (Cocalico Biologicals), resulting in anti-serum 1774. The *Rnf17l* cDNA fragment corresponding to the residues 1341-1540 was cloned into pQE30 (Qiagen). The 6×His-RNF17L (1341-1540) fusion protein was expressed in M15 bacteria, purified with Ni-NTA agarose, eluted in 8 M urea and used to immunize two guinea pigs (Cocalico Biologicals), resulting in anti-serum GP8. Specific antibodies were affinity-purified with the immunoblot method (Harlow and Lane, 1998).

Western blotting and co-immunoprecipitation

Adult testes were homogenized using a glass homogenizer in the SDS-PAGE sample buffer (100 mM Tris, pH 8.3, 2% SDS, 200 mM DTT, 10% glycerol, 1 mM EDTA, 0.025% bromophenol blue). Protein lysate (30 μg) was resolved on 9% SDS-PAGE gels and electro-blotted onto PVDF membranes. For some experiments, cytoplasmic and nuclear fractions of testis were prepared using the NE-PER kit according to the manufacturer's protocol (Pierce). Western blotting was performed using the following antibodies: anti-serum 1774 (1:500), anti-serum GP8 (1:500), anti-MVH (1:10,000), anti-SYCP3 (1:2,000) and anti-β-actin (1:2,500, Sigma). HRP-conjugated anti-rabbit or anti-guinea pig secondary antibodies (Sigma) were used.

For immunoprecipitation, one adult testis (80 mg) was homogenized in NP-40 lysis buffer [150 mM NaCl, 1.0% NP-40 and 50 mM Tris (pH 8.0)] in the presence of protease inhibitors (Sigma), incubated at 4°C for 30 minutes, and spun at 10,000 ***g*** for 10 minutes. The resulting supernatant was pre-cleared by incubation with 20 μl pre-bleed serum and 20 μl protein A agarose (Invitrogen) for 1 hour at 4°C and by centrifugation at 1000 ***g*** for 10 minutes. Subsequently, the supernatant was incubated with 20 μl anti-serum GP8 (RNF17L-specific) or pre-bleed at 4°C overnight, incubated with 20 μl protein A agarose for 1 hour, and spun at 10,000 ***g*** for 10 minutes. The pellets were washed with NP-40 lysis buffer five times and proteins were dissolved in 15 μl SDS-PAGE sample buffer. Immunoprecipitated proteins were subjected to western blot analysis with anti-serum 1774.

Immunofluorescence microscopy

Adult testes were fixed in fresh 4% paraformaldehyde (PFA) at 4°C overnight and were dehydrated in 30% (w/v) sucrose. The testes were embedded with TBS tissue freezing medium (Fisher Scientific) and frozen at temperatures below –20°C. Sections (8 μm) were cut using a Reichert-Jung cryo-microtome. Sections were post-fixed in 4% PFA at room temperature for 10 minutes prior to immunostaining. Primary antibodies used were as follows: anti-RNF17 (anti-sera 1774 and GP8), rat anti-TDRD1 (Chuma et al., 2003), rat anti-LAMP2 (GL2A7, Developmental Studies Hybridoma Bank) (Granger et al., 1990) and rat TRA54 monoclonal antibody (Pereira et al., 1998). Texas Red or FITC-conjugated secondary antibodies were used. Nuclear DNA was stained with DAPI. For immunostaining with anti-TDRD1 antibodies, the testis was fixed in 2% PFA for 30 minutes. Immunostained sections were visualized under a Zeiss Axioskop 40 fluorescence microscope. Images were captured with an Evolution QEi digital camera (MediaCybernetics) and processed with the Image-Pro software (Phase 3 Imaging Systems).

Immuno-electron microscopy (EM)

Immuno-EM was performed as described previously (Allen et al., 1996). Briefly, an adult testis was fixed in 2% PFA and 0.05% glutaraldehyde for 1 hour, washed with PBS, dehydrated with ethanol at –25°C, embedded in Lowicryl K4M medium, and polymerized with UV (365 nm) at –25°C for 5 days. Ultra-thin sections (100 nm) were

cut and collected on Formvar-coated Nickel grid. Ultra-thin sections were immunostained with anti-RNF17 antibodies or pre-bleed serum and 10 nm gold particle-conjugated secondary antibodies (Electron Microscopy Sciences), counterstained with uranyl acetate and lead citrate, and visualized with a JEOL-1010 electron microscope.

Cell culture and transfection

Rnf17 cDNAs were cloned in frame with GFP into pEGFP-C1 (BD Biosciences). NIH 3T3 cells were grown in D-MEM media supplemented with 10% newborn calf serum and transfected with various plasmids using Lipofectamine reagent (Invitrogen). Twenty-four to 48 hours after transfection, cells were washed twice with PBS, fixed in cold methanol for 15 minutes, air dried for 5 minutes, mounted with DAPI-containing Vectashield mounting medium (Vector Labs) and visualized on a Zeiss Axioskop 40 microscope.

GST-pulldown assay

The cDNA fragment corresponding to RNF17 (amino acids 1-287) was cloned into pGEX-4T-1. The GST-RNF17 (1-287) was expressed in BL21 bacteria and purified. The pGBKT7-RNF17 (amino acids 1-626) construct was used in a 50 μl reaction for in vitro transcription and translation in the presence of [^{35}S]methionine with the TNT kit (Promega). In vitro translated [^{35}S]RNF17 (1-626) (5 μl) was incubated with 2 μg of GST-RNF17 (1-287) or GST in a 100 μl reaction at RT for 30 minutes. A 50% (v/v) slurry of glutathione beads (20 μl) was added. After incubation for 30 minutes, beads were washed extensively with TNT buffer prior to addition of 15 μl SDS-PAGE sample buffer. Protein samples were resolved on 12% SDS-PAGE gels and were subject to autoradiography.

Generation of the *Rnf17* knockout mice

To make the targeting construct, we obtained five *Rnf17*-positive BAC clones by screening a 129Sv genomic DNA library (http://bacpac.chori.org/). One BAC clone (RPCI22-539M9) was used as the PCR template to amplify two homologous arms of 2.6 kb and 2.7 kb by using high-fidelity HF2 *Taq* DNA polymerase (BD Biosciences Clontech) and 25 cycles of PCR. The left arm (2.6 kb) lies 1 kb upstream of exon 1 and was subcloned into the *Eco*RI-digested pPGKNeo vector. The right arm consists of 2.7 kb of sequence immediately downstream of exon 2 and was subcloned into the *Sal*I site of the pPGKNeo vector (Fig. 7A). Sequencing of both arms revealed no mutations in the final targeting construct. The targeting construct was linearized with *Xho*I and electroporated into the V6.5 ES cells (Eggan et al., 2001). We recovered 384 clones following growth in G418 (350 μg/ml, Invitrogen). Three ES clones were homologously targeted at both 5′ and 3′ ends. We obtained chimera mice by injecting targeted ES clones into BALB/c blastocysts. PCR primers used for genotyping were as follows (Fig. 7A): P1, GTGGAGAGTAAGAGTGGAGC; P2, AAACTACCCAGGAAAATCAAGT; P3, CCGATGGGCTTTATTCTTAAC; P4, TCCTGACTAGGGGAGGAGTA. The PCR product of the wild-type allele assayed with P1 and P2 is 457 bp, and the PCR product of the mutant allele assayed with P3 and P4 is 250 bp (Fig. 7B). For histological analysis, testes were fixed in Bouin's solution and embedded in paraffin. Sections (6 μm) were stained with Hematoxylin/Eosin.

Northern blot analysis

Total RNAs were prepared from mouse tissues by using Trizol reagent (Invitrogen). Total RNAs (10 μg) from each tissue were separated on 2% agarose gel and blotted onto nitrocellulose membrane. After pre-hybridization in Rapid-hyb buffer (Amersham Biosciences), the membrane was hybridized with ^{32}P-labeled probes, washed and subjected to autoradiography. In Fig. 9B, the same set of membranes were stripped of probes and hybridized with different gene probes. The DNA probes were amplified from total testis cDNAs by RT-PCR using the following primers: *Rnf17* (bases 1-861), TACTCGAGCTATGGCGGCAGAGGCTTCGTC and AAGAATTCGATTACATGCAGATGGCCTCACTGCA; *Ldh3*, ACTGGATCCGGATCTGCAGTTATAAACTC and GACGAATTCGTGGTGGTTGCCTTTAATAC; *Miwi*, CTTCACCACCTCCATCCTTC and TCTGTTCTGTCATCCACCTC; *Pabpc3*, ACTGGATCCCTAGTGCAAAGGTAACGATG and GACGAATTCCCCTAACATTTGCTTTTGAG; *Tpap*, CAGCATACCCACAGCAGAAC and AGGTGGTGGTGAAATGGTAG. The primers for *Act*, *Crem*, *Prm1*, *Prm2*, *Tp1*, *Trf2* and β-actin have been previously described (Kashiwabara et al., 2002).

Results

Identification of two *Rnf17* isoforms

We examined expression of *Rnf17* in a panel of adult mouse tissues including testis and ovary by northern blot analysis. *Rnf17* was exclusively expressed in the testis (Fig. 1A). In

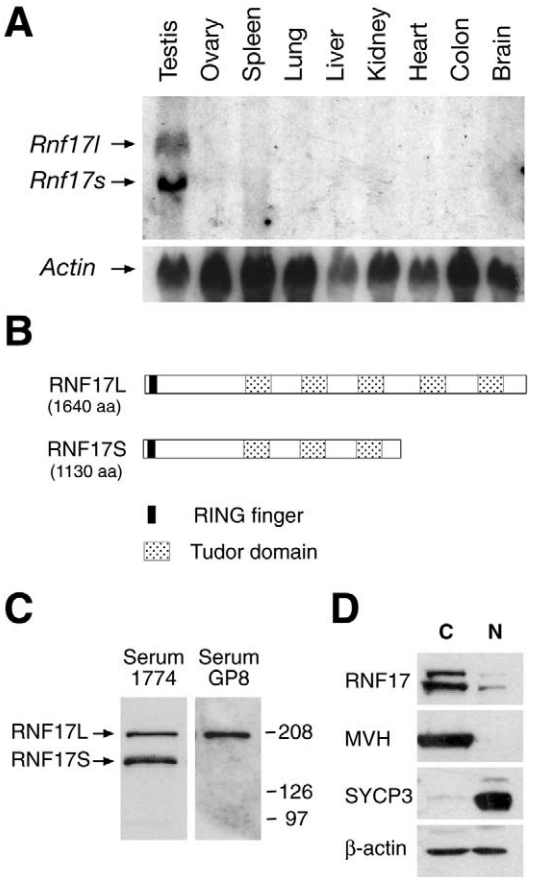

Fig. 1. Identification of two *Rnf17* isoforms. (A) Northern blot analysis of *Rnf17* expression. Two *Rnf17* transcripts (5.2 kb and 3.5 kb) were detected in the testis. β-Actin served as a loading control. (B) Schematic diagram of two RNF17 protein isoforms. (C) Western blot analysis of RNF17 proteins. Testicular protein extracts (30 μg) were resolved by SDS-PAGE. Anti-serum 1774 recognized both RNF17L and RNF17S. Anti-serum GP8 was specific to RNF17L. (D) RNF17 is largely cytoplasmic. Cytoplasmic and nuclear fractions of adult testis were prepared and subjected to western blot analysis. MVH (Mouse Vasa homolog) is a cytoplasmic protein control (Toyooka et al., 2000); SYCP3 (synaptonemal complex protein 3) is a nuclear protein control (Chuma and Nakatsuji, 2001); β-actin served as a loading control. C, cytoplasmic fractions; N, nuclear fractions.

addition, this analysis revealed two *Rnf17* transcripts, which were referred to as *Rnf17l* (5.2 kb) and *Rnf17s* (3.5 kb). These transcripts were much longer than previously reported (Wang et al., 2001; Yin et al., 1999). By using 3′-RACE, we obtained the composite sequences for both transcripts. Comparison of cDNA sequences with the mouse genomic sequence demonstrated that alternative splicing resulted in these two *Rnf17* transcripts, which shared the first 25 exons and differed only in their 3′ sequences. The last exon of *Rnf17s* (exon 26) contains a non-canonical polyadenylation signal (AATAA) and is AT rich. By contrast, the *Rnf17l* transcript lacks exon 26, contains 12 additional exons, and contains a canonical polyadenylation site (AATAAA) in its last exon.

Two RNF17 proteins were predicted from the new cDNA sequences (Fig. 1B). RNF17L (1640 amino acids) consists of a RING finger motif and five tudor domains. RNF17S (1130 amino acids) contains only three tudor domains. The RING finger is a zinc-binding motif. A growing number of RING-containing proteins were found to exhibit ubiquitin E3 ligase activities (Joazeiro and Weissman, 2000; Lorick et al., 1999). The 60 amino acid tudor domain was first identified in the *Drosophila* Tudor protein, which contains 10 copies.

RNF17 is a cytoplasmic protein in male germ cells

We raised polyclonal antibodies (anti-serum 1774) against the N-terminal 100 residues of RNF17. By western blot analysis, anti-serum 1774 recognized two bands with M_r of 200 kDa and 160 kDa in testis (Fig. 1C), which appeared to correspond to RNF17L and RNF17S. Both RNF17 isoforms migrated at a slower rate than expected, possibly owing to the high percentage of negatively charged residues (15%). RNF17S is more abundant than RNF17L. To distinguish between the two RNF17 isoforms, we generated polyclonal antibodies (anti-serum GP8) against the C-terminal region of RNF17L (residues 1341-1540). As expected, anti-serum GP8 recognized only RNF17L and not RNF17S. To determine the subcellular compartment to which RNF17 was localized, we prepared cytoplasmic and nuclear fractions of testicular protein extracts. Western blot analysis with anti-serum 1774 demonstrated that both RNF17L and RNF17S were present predominantly in the cytoplasm (Fig. 1D). They were also detected in the nucleus but in much lower abundance.

RNF17 is localized to a novel organelle

We next determined the subcellular localization of RNF17 by indirect immunofluorescence on testis sections using affinity-purified antibodies (anti-serum 1774). RNF17 was diffusely localized in the cytoplasm of all germ cells (spermatogonia, spermatocytes and spermatids) (Fig. 2). In addition, the RNF17 localization was exhibited as large perinuclear dots in some spermatocytes and spermatids but not in spermatogonia. It appeared that one prominent dot was present in each cell, but more than one dot could be present in spermatocytes. This dot-like structure was not previously reported, and thus we named it ‘RNF17 granule’.

The presence of RNF17 granules in germ cells is stage dependent. The mouse seminiferous tubules are classified into 12 stages (I-XII), each of which consists of a unique assortment of differentiating germ cells (Russell et al., 1990). The development of acrosomes in spermatids is closely correlated with each stage of spermatogenesis and therefore has been used as a major criterion for staging of seminiferous tubules. SP10 (Gene symbol: *Acrv1*) is a component of the acrosome (Reddi et al., 1995). To determine the appearance of RNF17 granules, we performed double immunostaining of adult testis sections with anti-RNF17 and anti-SP10 antibodies (Fig. 2). Staining of nuclei with DAPI further facilitated staging of seminiferous tubules. We did not observe RNF17 granules in early spermatocytes (pre-leptotene, leptotene and zygotene). However, small granules were present in the pachytene spermatocytes at stages II-VII (Fig. 2C,E). RNF17 granules appeared as large prominent dots in pachytene spermatocytes at stages VIII-X (arrows, Fig. 2G,I) and in diplotene spermatocytes at stage XI (arrow, Fig. 2K). We did not observe

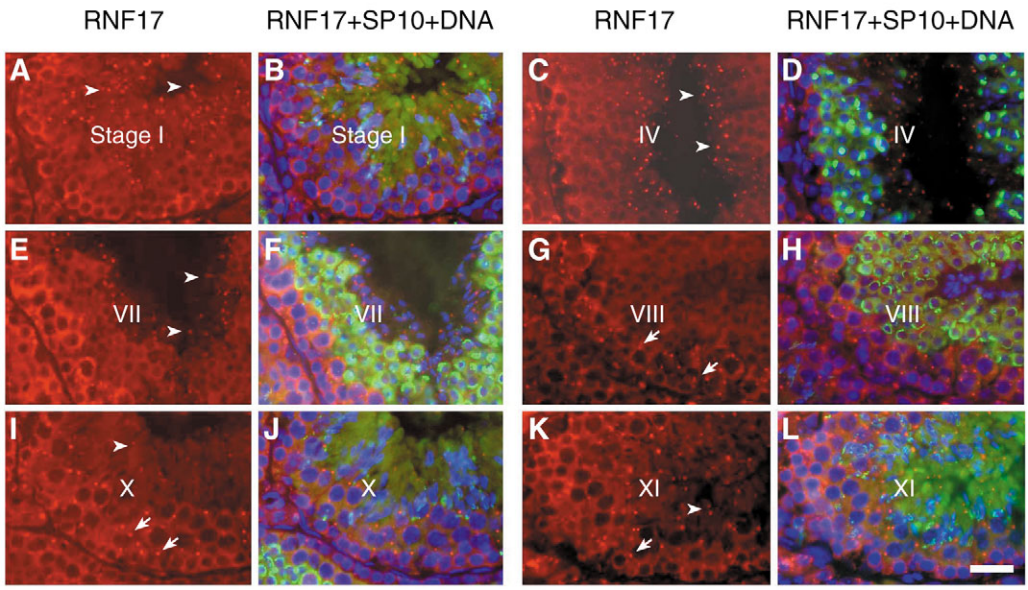

Fig. 2. Distribution of RNF17 in male germ cells. Sections of adult testis were immunostained with anti-RNF17 antibodies (anti-serum 1774, red). For purposes of staging, testis sections were also stained with anti-SP-10 antibodies (green) and counterstained with DAPI (blue). Only part of a seminiferous tubule is shown in each panel. Anti-RNF17 staining alone is shown in A,C,E,G,I,K. The merged image of anti-RNF17, anti-SP10 and DAPI is shown in B,D,F,H,J,L. The stage of each seminiferous tubule is indicated in the center. Representative RNF17 granules are indicated by arrows in pachytene or diplotene spermatocytes, or by arrowheads in elongating spermatids. Immunostaining of *Rnf17*-null testes with antiserum 1774 was negative (data not shown). Control experiments without primary antibodies were also negative (data not shown). Scale bar: 20 μm.

RNF17 granules in early spermatids (steps 1-9), which form the middle layers of germ cells with small round nuclei (step 1, Fig. 2A,B; step 4, Fig. 2C,D; step 7, Fig. 2E,F). RNF17 granules appeared again in step 10 spermatids (arrowhead, Fig. 2I) and became very prominent in spermatids of steps 11-16, indicated by arrowheads (step 11, Fig. 2K; step 13, Fig. 2A; step 15, Fig. 2C; step 16, Fig. 2E). In summary, RNF17 granules were observed in pachytene and diplotene spermatocytes at stages VIII-XI, disappeared in spermatids of steps 1-9 and were assembled again in spermatids of steps 10-16.

To distinguish the distribution of RNF17L and RNF17S, we performed double immunostaining of testis sections with anti-sera 1774 and GP8. Staining with anti-serum GP8 revealed that RNF17L was localized to granules in the pachytene and diplotene spermatocytes but not those in the spermatids (Fig. 3B,C). However, RNF17 granules in the spermatids were stained by anti-serum 1774 but not GP8, implying that they contain RNF17S but not RNF17L (Fig. 3C).

RNF17 granules are distinct organelles in male germ cells

The chromatoid body is a well-described nuage in mammalian germ cells (Fawcett et al., 1970; Sud, 1961a). To address whether RNF17 granules are chromatoid bodies, we performed colocalization studies with anti-RNF17 and anti-TDRD1 antibodies. TDRD1 is a known component of chromatoid bodies (Chuma et al., 2003). Precursors of chromatoid bodies appeared as numerous small punctate structures in spermatocytes (Fig. 4A). Only one large irregularly shaped chromatoid body was observed in each spermatid (Fig. 4B). The RNF17 granules recognized by anti-RNF17 antibodies were prominent in both spermatocytes and spermatids (Fig. 4A,B). Apparently, RNF17 did not colocalize with TDRD1. TDRD6 is another component of chromatoid bodies (S.C., unpublished). RNF17 did not colocalize with TDRD6 (data not shown). In conclusion, RNF17 granules were distinguishable from chromatoid bodies. TRA54 (a monoclonal antibody) recognizes cytoplasmic granules in round spermatids, in addition to Golgi apparatus and acrosome (Pereira et al., 1998; Ventela et al., 2003). We did not detect specific co-localization between RNF17 and TRA54, suggesting that RNF17 granules are distinct from TRA54-positive granules (data not shown).

Then we explored whether RNF17 granules might be lysosomes. Lysosomes are membrane-bound cytoplasmic organelles. LAMP2 (lysosome-associated membrane protein 2) is a component of lysosomes (Chen et al., 1985). We performed double immunostaining of testis sections with anti-RNF17 and anti-LAMP2 antibodies. We detected lysosomes in spermatids (Fig. 4D), but not in spermatocytes (Fig. 4C). We did not observe co-localization of RNF17 and LAMP2, and thus concluded that RNF17 granules are distinct from lysosomes.

RNF17 granules are spherical electron-dense structures

We performed ultrastructural analysis of RNF17 granules by immuno-electron microscopy (EM). Ultra-thin sections of the adult testis were probed with anti-RNF17 antibodies and gold-conjugated secondary antibodies. RNF17 granules were

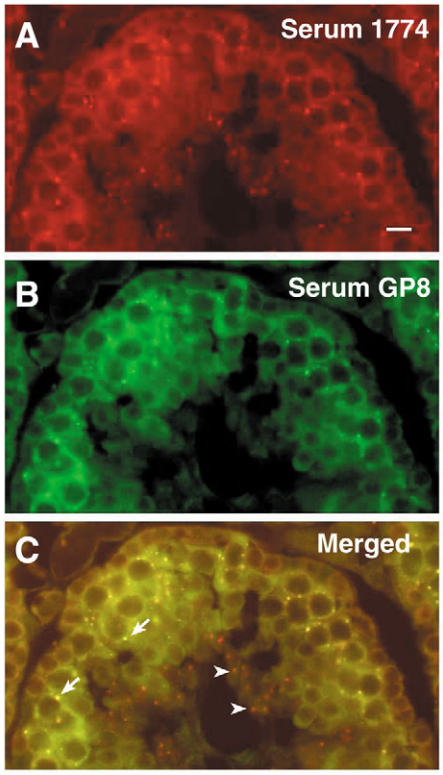

Fig. 3. Differential distribution of RNF17 protein isoforms. Adult testis sections were immunostained with anti-sera 1774 in red (A) and GP8 in green (B). The seminiferous tubule shown is in stage X. In the merged image (C), selected RNF17 granules are indicated by arrows in the spermatocytes, and by arrowheads in the spermatids. Scale bar: 10 μm.

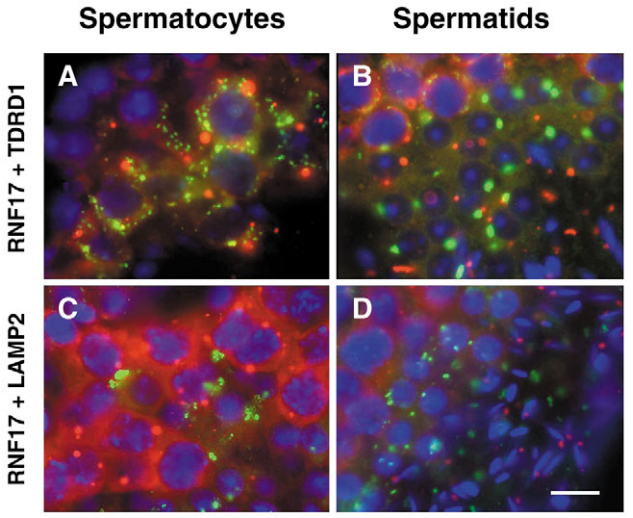

Fig. 4. RNF17 granules are distinct organelles in the testis. Double immunostaining of adult testis sections was performed with antiserum 1774 (red) and anti-TDRD1 antibodies (green) or anti-LAMP2 antibodies (green). RNF17 granules (red) are prominent in spermatocytes (A,C) and elongating spermatids (B,D). Dynamic changes of chromatoid bodies (green) are seen in spermatocytes (A) and spermatids (B). Lysosomes (green) are not present in spermatocytes (C) but are abundant in spermatids (D). Scale bar: 10 μm.

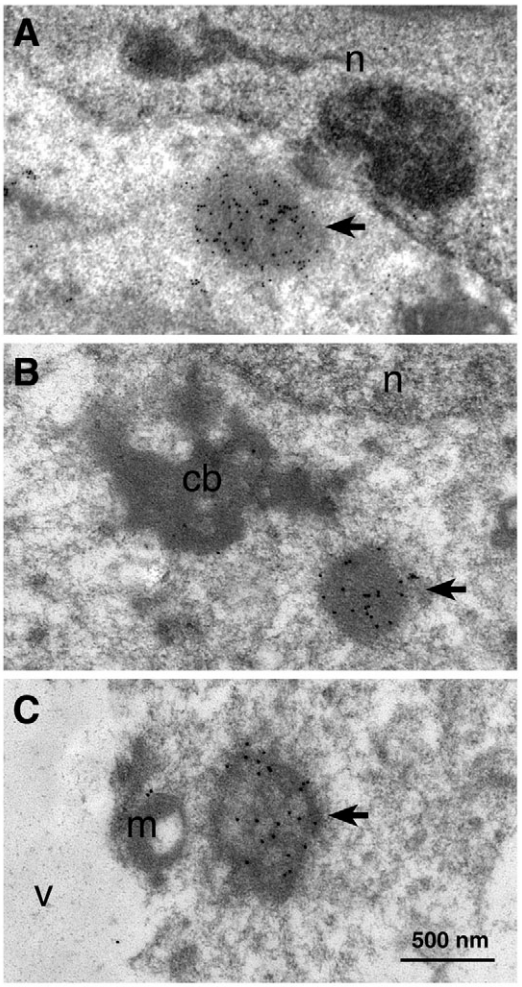

Fig. 5. Ultrastructural analysis of RNF17 granules by immuno-EM. Affinity purified anti-RNF17 antibodies (anti-serum 1774) were used as primary antibodies. Secondary antibodies were labeled with 10 nm gold particles. (A) The RNF17 granule in a spermatocyte. (B) The RNF17 granule in a spermatid. (C) The RNF17 granule in a cytoplasmic residual body. Arrows indicate the accumulation of gold particles in the 500 nm RNF17 granules. Immuno-EM without the primary antibody was negative (data not shown). cb, chromatoid body; m, mitochondria; n, nucleus; v, vacuole.

heavily labeled by gold particles (Fig. 5). The immuno-EM analysis showed that RNF17 granules are spherical electron-dense organelles with a diameter of 0.5 μm (Fig. 5), which is consistent with their manifestation as round dots in immunofluorescence studies (Fig. 2). Furthermore, RNF17 granules did not appear to be surrounded by membranes, but rather contained outwardly protruding fine fibers. Under EM, we frequently observed RNF17 granules in spermatocytes (Fig. 5A). RNF17 granules were also observed in spermatids (Fig. 5B). As expected, the irregularly shaped chromatoid body (cb) in the spermatid was not labeled with gold particles (Fig. 5B). RNF17 granules were found to be smaller than chromatoid bodies, which are 1-2 μm in diameter (Fawcett et al., 1970). Residual bodies are formed by the fusion of cytoplasmic materials shed by elongating spermatids (Russell et al., 1990). The residual bodies are characterized by the presence of vacuoles and lack of nucleus. RNF17 granules were observed in residual bodies, implying that at least some RNF17 granules are discarded by elongating spermatids (Fig. 5C).

RNF17 forms large granules in NIH 3T3 cells

To address whether RNF17 is able to form granules de novo, we expressed the GFP-RNF17L fusion protein in NIH 3T3 fibroblast cells. RNF17 was predominantly cytoplasmic and distributed in a punctate pattern (Fig. 6B), suggesting that RNF17 may form oligomers. The number and size of granules varied from cell to cell, possibly owing to different levels of protein expression. Furthermore, we observed the same punctate cytoplasmic localization pattern for GFP-RNF17L in two other cell lines: BHK21 hamster cells and immortalized GC-1spg germ cells (data not shown) (Hofmann et al., 1992).

To define the minimal region of RNF17 that is required for granule formation, a series of terminal truncations of RNF17 were generated and expressed in NIH 3T3 cells. Transfected cells were examined for RNF17 protein distribution by fluorescence microscopy. These experiments demonstrated that the 45-amino acid region of RNF17 (residues 243-287) is both necessary and sufficient for granule formation (Fig. 6A). Without this region, the distribution of RNF17 displayed a diffuse pattern (Fig. 6B). These data suggest that the 45-amino acid RNF17 (243-287) region, referred to as the binding domain, might be involved in dimerization or polymerization of RNF17.

RNF17 associates with itself both in vivo and in vitro

To determine whether RNF17 is associated with itself in vivo, we took advantage of the presence of two RNF17 isoforms. RNF17L and its associated proteins were immunoprecipitated from the total testis protein extract with RNF17L-specific antibodies (anti-serum GP8) and were subject to western blot analysis with anti-serum 1774. Our co-immunoprecipitation experiment showed that RNF17L and RNF17S were associated with each other in vivo (Fig. 6C).

We next performed GST pulldown experiments to determine whether RNF17 physically binds to itself. Our GST pulldown experiment showed that in vitro translated RNF17 (1-626) was able to bind to GST-RNF17 (residues 1-287) but not GST, suggesting that RNF17 physically interacts with itself (Fig. 6D). We further confirmed the interaction by yeast two-hybrid assay (data not shown).

Generation of mice lacking *Rnf17*

To investigate the function of *Rnf17* in spermatogenesis, we used homologous recombination in embryonic stem cells to create mice that lack the *Rnf17* gene. In the targeting construct, a 4.1 kb DNA fragment containing the first two exons of *Rnf17* was replaced by the neomycin selection marker (Fig. 7A). This *Rnf17* mutant allele deletes the ATG initiation codon, the RING finger and part of its Mad-binding domain (Wang et al., 2001; Yin et al., 1999). The RNF17 protein was not detected in $Rnf17^{-/-}$ testis by western blotting, indicating that an *Rnf17*-null mutant was generated (Fig. 7C).

Spermiogenesis deficiency in the *Rnf17* mutant mice

Rnf17-deficient mice appear to be normal in development. No gross defects have been observed up to 8 months of age. Interbreeding of heterozygous ($Rnf17^{+/-}$) mice yielded the

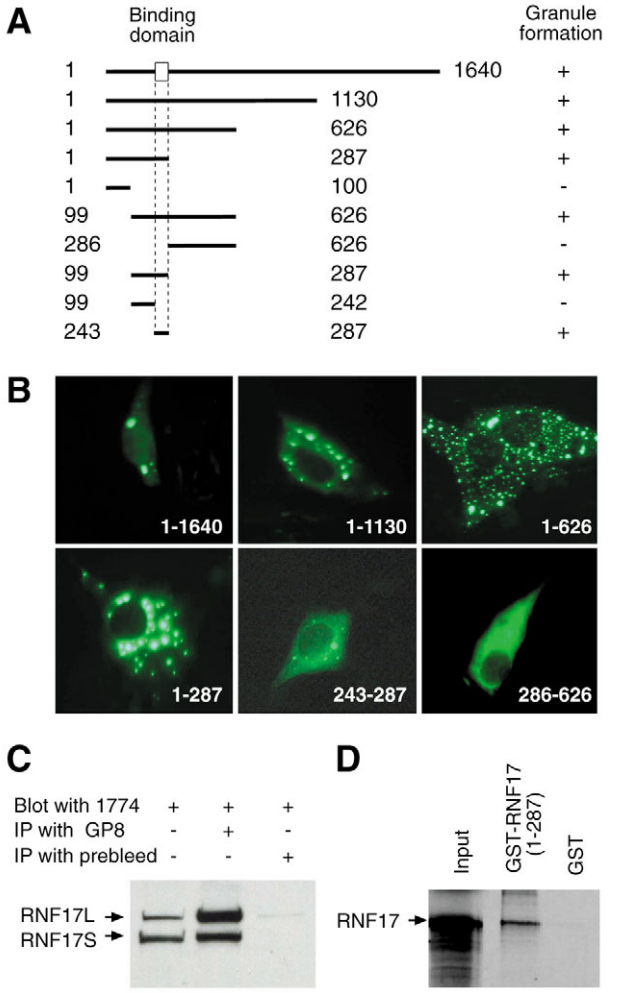

Fig. 6. RNF17 binds to itself both in vivo and in vitro. (A) Identification of the RNF17 granule formation domain. Truncated RNF17 polypeptides were expressed as GFP fusion proteins in NIH 3T3 cells. Formation of granules was assayed by fluorescence microscopy. +, formation of GFP-RNF17 granules; –, diffuse GFP-RNF17 distribution. The numbers adjacent to the endpoints designate the corresponding amino acid positions. (B) Distribution of GFP-fusion proteins expressed in NIH 3T3 cells. Punctate granules were present in cells expressing RNF17L (1-1640), RNF17S (1-1130), RNF17 (1-626), RNF17 (1-287) or RNF17 (243-287). RNF17 (286-626) or GFP alone (data not shown) was diffusely distributed. (C) Co-immunoprecipitation of RNF17L and RNF17S from testis. Immunoprecipitation (IP) using testis protein extracts was carried out with RNF17L-specific antibodies (anti-serum GP8). Immunoprecipitated proteins were subjected to western blot analysis with anti-serum 1774. IP with pre-bleed serum served as a control. (D) GST-pulldown assay. GST-RNF17 (1-287) was expressed in *E. coli* and purified with glutathione beads. RNF17 (1-626) was in vitro translated in the presence of [^{35}S]methionine. GST alone served as a control.

Mendelian ratio (77:164:78) of $Rnf17^{+/+}$, $Rnf17^{+/-}$ and $Rnf17^{-/-}$ offspring, suggesting that disruption of *Rnf17* causes no embryonic lethality. The $Rnf17^{-/-}$ males were infertile, despite normal sexual behavior, as evidenced by formation of copulatory plugs in females. By contrast, $Rnf17^{-/-}$ females exhibited normal fertility and produced normal litter sizes

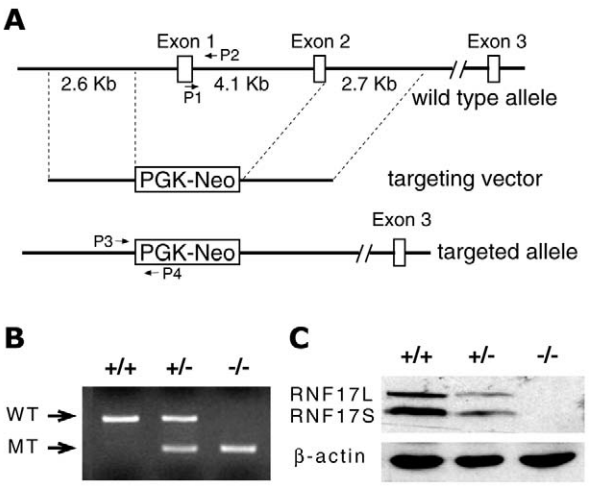

Fig. 7. Targeted disruption of the *Rnf17* gene. (A) Schematic diagram of the wild-type allele, the targeting vector and the targeted allele. PGK-Neo: neomycin-resistance gene driven by the *PGK1* promoter. PCR primers (P1, P2, P3 and P4) used for genotyping are indicated. (B) PCR analysis of genomic DNA from *Rnf17* mice. +/+, wild type; +/–, heterozygote; –/–, homozygote. All four primers were included in each PCR assay. WT, wild-type allele; MT, mutant allele. (C) Absence of RNF17 proteins in the *Rnf17*-deficient testes. Western blot analysis was done with both anti-sera 1774 (as shown) and GP8 (data not shown).

(7.0±1.1 offspring, n=7 litters). Histological analysis of $Rnf17^{-/-}$ ovaries revealed no abnormalities.

Testes of 8-week-old $Rnf17^{-/-}$ mice were 25% smaller than those of wild-type littermates. Histology revealed that the diameter of seminiferous tubules was significantly smaller in $Rnf17^{-/-}$ testis (Fig. 8B) than in wild type (Fig. 8A). In adult $Rnf17^{-/-}$ testis, Leydig cells and Sertoli cells appeared to be normal in number, size and morphology. However, while germ cells developed to round spermatids, they then failed to differentiate into elongating spermatids (Fig. 8D), demonstrating that *Rnf17* is required for spermiogenesis. Round spermatids first begin to differentiate into elongating forms 28 days after birth. Testes from $Rnf17^{-/-}$ mice at day 28 after birth and beyond contained round spermatids but lacked elongating spermatids completely, suggesting that *Rnf17* is also essential for spermiogenesis in the first wave of spermatogenesis. Immunostaining of acrosomes with anti-SP10 antibodies revealed that round spermatids advanced up to step 4 in *Rnf17*-deficient testis (Fig. 8H).

In the seminiferous tubules of $Rnf17^{-/-}$ testes, we frequently observed large multi-nucleated degenerating cells, which we believed to be apoptotic cells (Fig. 8D). Such large abnormal cells were rarely seen in normal testes. Interestingly, epididymal tubules from 8-week-old wild-type mice were filled with sperm (Fig. 8E), whereas those from $Rnf17^{-/-}$ mice contained apparently apoptotic round spermatids (Fig. 8F). No sperm were found in the epididymis of $Rnf17^{-/-}$ mice, which accounts for their infertility.

Downregulation of spermiogenesis genes in *Rnf17*-null testis

To identify potential downstream target genes of *Rnf17*, we performed Northern blot analysis of known testis-specific

genes in *Rnf17*$^{-/-}$ testis. A number of genes that begin to transcribe in meiosis, such as *Ldh3* (lactate dehydrogenase 3, C chain), *Miwi* and *Pabpc3* (poly A-binding protein, cytoplasmic 3), did not show significantly reduced expression in *Rnf17*$^{-/-}$ testis when compared with wild-type and *Rnf17*$^{+/-}$ testes (Fig. 9A) (Deng and Lin, 2002; Sakai et al., 1987; Wang et al., 1992). However, genes that initiate transcription postmeiotically, such as *Act* (activator of CREM in testis), *Tp1* (transition protein 1), *Prm1* (protamine 1) and *Prm2* (protamine 2), exhibited greatly reduced expression in *Rnf17*$^{-/-}$ testis (Fig. 9A). These expression data are consistent with the spermiogenic defects in *Rnf17*$^{-/-}$ testes revealed by histology.

To determine whether the reduced expression of postmeiotic genes in *Rnf17*-deficient mice is due to transcriptional regulation by *Rnf17* or to the absence of elongating spermatids, we examined gene expression in juvenile testes from different developmental stages. We observed significant reduction in the expression of *Act*, *Tp1*, *Prm1* and *Prm2* in *Rnf17*$^{-/-}$ testes of 24 days after birth, when the most differentiated germ cells are round spermatids (Fig. 9B). This reduction cannot be explained by a lack of elongating spermatids in *Rnf17*$^{-/-}$ testes, as such cells do not appear in normal testes until day 28. By contrast, the level of expression of *Ldh3* is indistinguishable between *Rnf17*$^{-/-}$ and wild-type testes throughout development. In addition, we examined expression of four known key regulators of spermiogenesis (*Crem*, *Trf2*, *Miwi* and *Tpap*) to address whether their expression might be regulated by *Rnf17*. Expression of these four genes is comparable in *Rnf17*$^{-/-}$ and wild-type testes, suggesting that *Rnf17* regulates spermiogenesis in a manner independent of these four known key regulators.

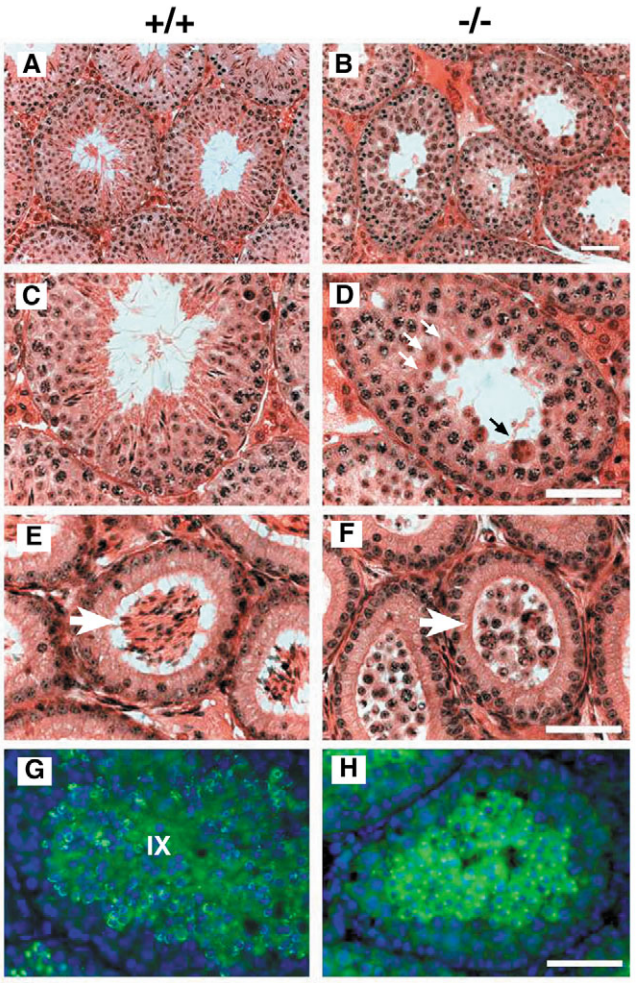

Fig. 8. Spermiogenesis defects in *Rnf17*-deficient mice. (A,B) Histological analysis of seminiferous tubules in adult wild-type (A) and *Rnf17*$^{-/-}$ (B) mice at low magnifications. (C,D) Histology of wild-type and *Rnf17*$^{-/-}$ seminiferous tubules at high magnifications. White arrows, round spermatids; black arrow, an abnormal multinucleated cell. (E) Wild-type epididymal tubules (arrow) are filled with sperm. (F) Epididymal tubules (arrow) from *Rnf17*$^{-/-}$ mice lack sperm but contain spermatid-like germ cells. (G,H) Acrosomal morphology in wild-type (Stage IX) and *Rnf17*-deficient seminiferous tubules. Testis sections were immunostained with anti-SP10 antibodies (green) and DNA was stained with DAPI (blue). Scale bars: 25 μm.

Discussion

Many types of nuage have been found in both male and female germ cells of a wide variety of species by electron microscopy (al-Mukhtar and Webb, 1971; Eddy, 1974; Sud, 1961a). It has

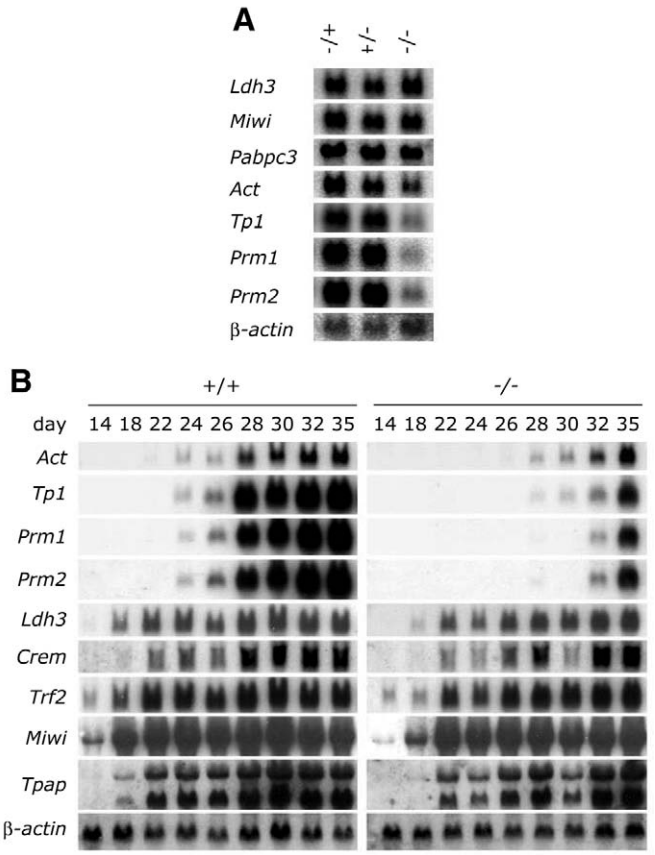

Fig. 9. Analysis of gene expression in *Rnf17*$^{-/-}$ testes. β-Actin was included as a control for RNA loading. (A) Northern blots of testis-specific genes in adult testes. +/+, wild type; +/–, heterozygote; –/–, homozygote. (B) Gene expression during juvenile testis development. Five testis-specific genes (*Act*, *Tp1*, *Prm1*, *Prm2* and *Ldh3*) and four key regulators of spermiogenesis (*Crem*, *Trf2*, *Miwi* and *Tpap*) were examined. The age of mice (in days after birth) is indicated. +/+, wild type; –/–, *Rnf17* deficient.

been hypothesized that nuages play important roles in germ cell specification and differentiation. Owing to a lack of specific markers, it has been difficult to identify and distinguish most nuages unambiguously. In this report, we definitively identify a novel mouse nuage, the RNF17 granule, and its first protein component. RNF17 granules appear to be distinguishable from other known germ cell nuages. TDRD1 is a component of the well-described chromatoid body in the male germ cells (Chuma et al., 2003). Our double immunostaining experiments demonstrated that RNF17 granules were distinct from chromatoid bodies. A spherical nuage was previously reported to be in contact with or close proximity to the chromatoid body and thus was referred to as the chromatoid satellite (Fawcett et al., 1970; Sud, 1961b). Chromatoid satellites are smaller and less electron dense than chromatoid bodies (Fawcett et al., 1970). Because we did not observe close association of RNF17 granules with chromatoid bodies, we reasoned that RNF17 granules were unlikely to be chromatoid satellites.

In addition to chromatoid bodies and chromatoid satellites, at least four different types of nuage were identified in rat spermatocytes by electron microscopy: 70-90 nm spherical particles, sponge bodies, inter-mitochondrial substance and 30 nm particles (Eddy, 1974; Russell and Frank, 1978). The appearance and dissociation of all six types of nuage are dynamic. However, except for chromatoid bodies, no cytological markers are known for the remaining five types of nuage, making it difficult to track these dynamically changing organelles definitively. Among these different types of nuage, the sponge body closely resembles the RNF17 granule in appearance and size. Sponge bodies in rats were large structures with a diameter of 0.5-1.5 μm. They appeared in late pachytene spermatocytes and were only occasionally seen in round spermatids. It was not reported if sponge bodies were present in elongating spermatids (Russell and Frank, 1978). RNF17 granules are very prominent in elongating spermatids in mice. However, the presence of sponge bodies in mice has not been reported. Whether RNF17 granules and sponge bodies represent the same structure remains to be examined.

Our data suggest that RNF17 may play a role in the assembly of RNF17 granules. Several lines of evidence support this notion. First, RNF17 physically bound to itself in the GST-pulldown assay. Second, RNF17L and RNF17S were co-immunoprecipitated from the testis, suggesting that they may form heterodimers. RNF17 granules in elongating spermatids contained RNF17S but not RNF17L, suggesting the possibility of RNF17S homodimerization. Third, RNF17 was capable of forming large aggregates when ectopically expressed in cultured cells. RNF17 aggregates have also been observed previously (Yin et al., 1999). Taken together, we hypothesize that RNF17 may form high order polymers in vivo and play a crucial role in the assembly of RNF17 granules.

RNF17 contains multiple tudor domains (Fig. 1). The specific functions of tudor domains remain elusive. However, two recent studies have shown that tudor domains are directly involved in protein-protein interactions. The tudor domain in SMN (survival of motor neuron) binds to Sm proteins of snRNP (small nuclear ribonucleoproteins) (Selenko et al., 2001). The tudor domain in 53BP1 (p53 binding protein 1) interacts with methylated histone 3 (Huyen et al., 2004). We hypothesize that the tudor domains in RNF17 may recruit other proteins to form large macromolecular complexes. Interestingly, the founding member of the tudor domain-containing protein, Tudor, is a component of polar granules in *Drosophila* and is required for their assembly (Bardsley et al., 1993). TDRD1/MTR-1 is a component of chromatoid bodies in mice (Chuma et al., 2003). TDRD6 is also a component of chromatoid bodies (S.C., unpublished). The localization of proteins with multiple tudor domains in nuages indicates a conserved role for tudor domains in these diverse organelles.

The chromatoid body has been assumed to serve as a storage site for proteins and RNAs during spermatid differentiation. A number of proteins and RNAs were found in chromatoid bodies, including TDRD1, MVH, DDX25, mRNAs and rRNAs (Chuma et al., 2003; Figueroa and Burzio, 1998; Toyooka et al., 2000; Tsai-Morris et al., 2004). However, the specific functions of chromatoid bodies remain unclear. Vasa is a highly conserved germ-cell-specific RNA helicase. Because targeted deletion of *Mvh* (mouse Vasa homolog) in mice resulted in meiotic arrest, the functional significance of the association of MVH with chromatoid body could not be studied (Tanaka et al., 2000). DDX25 is a gonadotropin-regulated testicular RNA helicase. In *Ddx25* mutant mice, spermatogenesis was blocked in the round spermatid stage, and chromatoid bodies in spermatids were markedly reduced in size, suggesting that chromatoid bodies may be essential for spermatid differentiation (Tsai-Morris et al., 2004). Chromatoid bodies were observed to travel between spermatids through cytoplasmic bridges and thus were proposed to be involved in sharing of haploid gene products between spermatids (Ventela et al., 2003). It is worth noting that chromatoid bodies are present in round spermatids, while RNF17 granules are present in late pachytene spermatocytes and elongating spermatids. The functions of these two nuages may be complementary during spermatogenesis. Analogous to chromatoid bodies, we assume that RNF17 granules may serve as a storage site for other proteins and RNAs, and may shuttle between interconnected germ cells to promote synchronized differentiation.

RNF17 binds to all four members of the Mad protein family (Mad1, Mxi1, Mad3 and Mad4), which are present in many tissues (Yin et al., 1999). Although *Rnf17* is required for spermiogenesis, mice lacking *Mad1*, *Mxi1* or *Mad3* are viable and fertile, suggesting functional redundancy among Mad proteins (Foley et al., 1998; Queva et al., 2001; Schreiber-Agus et al., 1998). As antagonists of Myc, Mad proteins repress transcription of Myc-responsive genes by competing with Myc for binding to the Max transcription factor (Grandori et al., 2000). RNF17 was shown to activate transcription of Myc-responsive genes by retaining Mad proteins in the cytoplasm (Yin et al., 2001; Yin et al., 1999). RNF17 is predominantly cytoplasmic in germ cells. It is possible that RNF17 sequesters Mad proteins in the cytoplasm and thereby prevents transcriptional repression of spermiogenesis-specific genes.

RNF17 is evolutionarily conserved in mammals. The RNF17L ortholog was identified in silico in the rat genome. A full-length cDNA clone encoding the human RNF17L ortholog was present in the public database. We observed RNF17 granules in the rat testis using our anti-RNF17 antibodies (data not shown), suggesting that RNF17 granules may be present in other mammalian species. RNF17 is a novel key regulator of spermiogenesis in mice. Therefore, we anticipate that the

essential role of RNF17 in spermiogenesis is conserved in other species, including humans.

We thank Q. C. Yu for Immuno-EM; R. Jaenisch for ES cells; P. Reddi for anti-SP10 antibodies; T. Noce for anti-MVH antibodies; H. Tanaka and Y. Nishimune for TRA54 antibody; DSHB (Developmental Studies Hybridoma Bank) for anti-LAMP2 antibodies; and Y. Cheng, G. L. Gerton, S. B. Moss, E. Gleason, B. Willenbring and F. Yang for comments on the manuscript. This work was supported by an NICHD grant (HD 045866 to P.J.W.).

References

al-Mukhtar, K. A. and Webb, A. C. (1971). An ultrastructural study of primordial germ cells, oogonia and early oocytes in Xenopus laevis. *J. Embryol. Exp. Morphol.* **26**, 195-217.

Allen, E., Yu, Q. C. and Fuchs, E. (1996). Mice expressing a mutant desmosomal cadherin exhibit abnormalities in desmosomes, proliferation, and epidermal differentiation. *J. Cell Biol.* **133**, 1367-1382.

Bardsley, A., McDonald, K. and Boswell, R. E. (1993). Distribution of tudor protein in the Drosophila embryo suggests separation of functions based on site of localization. *Development* **119**, 207-219.

Blendy, J. A., Kaestner, K. H., Weinbauer, G. F., Nieschlag, E. and Schutz, G. (1996). Severe impairment of spermatogenesis in mice lacking the CREM gene. *Nature* **380**, 162-165.

Chen, J. W., Murphy, T. L., Willingham, M. C., Pastan, I. and August, J. T. (1985). Identification of two lysosomal membrane glycoproteins. *J. Cell Biol.* **101**, 85-95.

Chuma, S. and Nakatsuji, N. (2001). Autonomous transition into meiosis of mouse fetal germ cells in vitro and its inhibition by gp130-mediated signaling. *Dev. Biol.* **229**, 468-479.

Chuma, S., Hiyoshi, M., Yamamoto, A., Hosokawa, M., Takamune, K. and Nakatsuji, N. (2003). Mouse Tudor Repeat-1 (MTR-1) is a novel component of chromatoid bodies/nuages in male germ cells and forms a complex with snRNPs. *Mech. Dev.* **120**, 979-990.

Deng, W. and Lin, H. (2002). miwi, a murine homolog of piwi, encodes a cytoplasmic protein essential for spermatogenesis. *Dev. Cell* **2**, 819-830.

Eddy, E. M. (1970). Cytochemical observations on the chromatoid body of the male germ cells. *Biol. Reprod.* **2**, 114-128.

Eddy, E. M. (1974). Fine structural observations on the form and distribution of nuage in germ cells of the rat. *Anat. Rec.* **178**, 731-757.

Eggan, K., Akutsu, H., Loring, J., Jackson-Grusby, L., Klemm, M., Rideout, W. M., 3rd, Yanagimachi, R. and Jaenisch, R. (2001). Hybrid vigor, fetal overgrowth, and viability of mice derived by nuclear cloning and tetraploid embryo complementation. *Proc. Natl. Acad. Sci. USA* **98**, 6209-6214.

Fawcett, D. W., Ito, S. and Slautterback, D. (1959). The occurrence of intercellular bridges in groups of cells exhibiting synchronous differentiation. *J. Biophys. Biochem. Cytol.* **5**, 453-460.

Fawcett, D. W., Eddy, E. M. and Phillips, D. M. (1970). Observations on the fine structure and relationships of the chromatoid body in mammalian spermatogenesis. *Biol. Reprod.* **2**, 129-153.

Figueroa, J. and Burzio, L. O. (1998). Polysome-like structures in the chromatoid body of rat spermatids. *Cell Tissue Res.* **291**, 575-579.

Foley, K. P., McArthur, G. A., Queva, C., Hurlin, P. J., Soriano, P. and Eisenman, R. N. (1998). Targeted disruption of the MYC antagonist MAD1 inhibits cell cycle exit during granulocyte differentiation. *EMBO J.* **17**, 774-785.

Grandori, C., Cowley, S. M., James, L. P. and Eisenman, R. N. (2000). The Myc/Max/Mad network and the transcriptional control of cell behavior. *Annu. Rev. Cell Dev. Biol.* **16**, 653-699.

Granger, B. L., Green, S. A., Gabel, C. A., Howe, C. L., Mellman, I. and Helenius, A. (1990). Characterization and cloning of lgp110, a lysosomal membrane glycoprotein from mouse and rat cells. *J. Biol. Chem.* **265**, 12036-12043.

Harlow, E. and Lane, D. (1998). *Using Antibodies: A Laboratory Manual.* Cold Spring Harbor: Cold Spring Harbor Laboratory Press.

Hay, B., Jan, L. Y. and Jan, Y. N. (1988). A protein component of Drosophila polar granules is encoded by vasa and has extensive sequence similarity to ATP-dependent helicases. *Cell* **55**, 577-587.

Hofmann, M. C., Narisawa, S., Hess, R. A. and Millan, J. L. (1992). Immortalization of germ cells and somatic testicular cells using the SV40 large T antigen. *Exp. Cell Res.* **201**, 417-435.

Huyen, Y., Zgheib, O., Ditullio, R. A., Jr, Gorgoulis, V. G., Zacharatos, P., Petty, T. J., Sheston, E. A., Mellert, H. S., Stavridi, E. S. and Halazonetis, T. D. (2004). Methylated lysine 79 of histone H3 targets 53BP1 to DNA double-strand breaks. *Nature* **432**, 406-411.

Joazeiro, C. A. and Weissman, A. M. (2000). RING finger proteins: mediators of ubiquitin ligase activity. *Cell* **102**, 549-552.

Kashiwabara, S., Noguchi, J., Zhuang, T., Ohmura, K., Honda, A., Sugiura, S., Miyamoto, K., Takahashi, S., Inoue, K., Ogura, A. et al. (2002). Regulation of spermatogenesis by testis-specific, cytoplasmic poly(A) polymerase TPAP. *Science* **298**, 1999-2002.

Lorick, K. L., Jensen, J. P., Fang, S., Ong, A. M., Hatakeyama, S. and Weissman, A. M. (1999). RING fingers mediate ubiquitin-conjugating enzyme (E2)-dependent ubiquitination. *Proc. Natl. Acad. Sci. USA* **96**, 11364-11369.

Mahowald, A. P. (1968). Polar granules of Drosophila. II. Ultrastructural changes during early embryogenesis. *J. Exp. Zool.* **167**, 237-261.

Mahowald, A. P. (2001). Assembly of the Drosophila germ plasm. *Int. Rev. Cytol.* **203**, 187-213.

Martianov, I., Fimia, G. M., Dierich, A., Parvinen, M., Sassone-Corsi, P. and Davidson, I. (2001). Late arrest of spermiogenesis and germ cell apoptosis in mice lacking the TBP-like TLF/TRF2 gene. *Mol. Cell* **7**, 509-515.

Nantel, F., Monaco, L., Foulkes, N. S., Masquilier, D., LeMeur, M., Henriksen, K., Dierich, A., Parvinen, M. and Sassone-Corsi, P. (1996). Spermiogenesis deficiency and germ-cell apoptosis in CREM-mutant mice. *Nature* **380**, 159-162.

Pereira, L. A., Tanaka, H., Nagata, Y., Sawada, K., Mori, H., Chimelli, L. M. and Nishimune, Y. (1998). Characterization and expression of a stage specific antigen by monoclonal antibody TRA54 in testicular germ cells. *Int. J. Androl.* **21**, 34-40.

Ponting, C. P. (1997). Tudor domains in proteins that interact with RNA. *Trends Biochem. Sci.* **22**, 51-52.

Queva, C., McArthur, G. A., Iritani, B. M. and Eisenman, R. N. (2001). Targeted deletion of the S-phase-specific Myc antagonist Mad3 sensitizes neuronal and lymphoid cells to radiation-induced apoptosis. *Mol. Cell. Biol.* **21**, 703-712.

Reddi, P. P., Naaby-Hansen, S., Aguolnik, I., Tsai, J. Y., Silver, L. M., Flickinger, C. J. and Herr, J. C. (1995). Complementary deoxyribonucleic acid cloning and characterization of mSP-10: the mouse homologue of human acrosomal protein SP-10. *Biol. Reprod.* **53**, 873-881.

Russell, L. and Frank, B. (1978). Ultrastructural characterization of nuage in spermatocytes of the rat testis. *Anat. Rec.* **190**, 79-97.

Russell, L. D., Ettlin, R. A., Sinha Hikim, A. P. and Clegg, E. D. (1990). *Histological and Histopathological Evaluation of the Testis*. Clearwater, Florida: Cache River Press.

Sakai, I., Sharief, F. S. and Li, S. S. (1987). Molecular cloning and nucleotide sequence of the cDNA for sperm-specific lactate dehydrogenase-C from mouse. *Biochem. J.* **242**, 619-622.

Schreiber-Agus, N., Meng, Y., Hoang, T., Hou, H., Jr, Chen, K., Greenberg, R., Cordon-Cardo, C., Lee, H. W. and DePinho, R. A. (1998). Role of Mxi1 in ageing organ systems and the regulation of normal and neoplastic growth. *Nature* **393**, 483-487.

Schultz, N., Hamra, F. K. and Garbers, D. L. (2003). A multitude of genes expressed solely in meiotic or postmeiotic spermatogenic cells offers a myriad of contraceptive targets. *Proc. Natl. Acad. Sci. USA* **100**, 12201-12206.

Selenko, P., Sprangers, R., Stier, G., Buhler, D., Fischer, U. and Sattler, M. (2001). SMN tudor domain structure and its interaction with the Sm proteins. *Nat. Struct. Biol.* **8**, 27-31.

Sharpe, R. M. (1993). *Regulation of Spermatogenesis. In The Physiology of Reproduction*, Vol. 1 (ed. E. Knobil and J. D. Neill), pp. 1363-1434. New York: Raven Press.

Shima, J. E., McLean, D. J., McCarrey, J. R. and Griswold, M. D. (2004). The murine testicular transcriptome: characterizing gene expression in the testis during the progression of spermatogenesis. *Biol. Reprod.* **71**, 319-330.

Sud, B. N. (1961a). The chromatoid body in spermatogenesis. *Quart. J. Microscop. Sci.* **102**, 273-292.

Sud, B. N. (1961b). Morphological and histochemical studies of the chromatoid body and related elements in the spermatogenesis of the rat. *Quart. J. Microscop. Sci.* **102**, 495-505.

Tanaka, S. S., Toyooka, Y., Akasu, R., Katoh-Fukui, Y., Nakahara, Y., Suzuki, R., Yokoyama, M. and Noce, T. (2000). The mouse homolog of Drosophila Vasa is required for the development of male germ cells. *Genes Dev.* **14**, 841-853.

Thomson, T. and Lasko, P. (2004). Drosophila tudor is essential for polar granule assembly and pole cell specification, but not for posterior patterning. *Genesis* **40**, 164-170.

Toyooka, Y., Tsunekawa, N., Takahashi, Y., Matsui, Y., Satoh, M. and Noce, T. (2000). Expression and intracellular localization of mouse Vasa-homologue protein during germ cell development. *Mech. Dev.* **93**, 139-149.

Tsai-Morris, C. H., Sheng, Y., Lee, E., Lei, K. J. and Dufau, M. L. (2004). Gonadotropin-regulated testicular RNA helicase (GRTH/Ddx25) is essential for spermatid development and completion of spermatogenesis. *Proc. Natl. Acad. Sci. USA* **101**, 6373-6378.

Ventela, S., Toppari, J. and Parvinen, M. (2003). Intercellular organelle traffic through cytoplasmic bridges in early spermatids of the rat: mechanisms of haploid gene product sharing. *Mol. Biol. Cell* **14**, 2768-2780.

Wang, M. Y., Cutler, M., Karimpour, I. and Kleene, K. C. (1992). Nucleotide sequence of a mouse testis poly(A) binding protein cDNA. *Nucleic Acids Res.* **20**, 3519.

Wang, P. J., McCarrey, J. R., Yang, F. and Page, D. C. (2001). An abundance of X-linked genes expressed in spermatogonia. *Nat. Genet.* **27**, 422-426.

Yin, X. Y., Gupta, K., Han, W. P., Levitan, E. S. and Prochownik, E. V. (1999). Mmip-2, a novel RING finger protein that interacts with mad members of the Myc oncoprotein network. *Oncogene* **18**, 6621-6634.

Yin, X. Y., Grove, L. E. and Prochownik, E. V. (2001). Mmip-2/Rnf-17 enhances c-Myc function and regulates some target genes in common with glucocorticoid hormones. *Oncogene* **20**, 2908-2917.

Zhang, D., Penttila, T. L., Morris, P. L., Teichmann, M. and Roeder, R. G. (2001). Spermiogenesis deficiency in mice lacking the *Trf2* gene. *Science* **292**, 1153-1155.